

Magneto-optical properties of two dimensional photonic crystals

A.K. Zvezdin and V.I. Belotelov^a

General Physics Institute of the Russian Academy of Sciences, 119991, Vavilov38, Moscow, Russia
and

M.V. Lomonosov Moscow State University, Faculty of Physics, 119992, Vorobievski gori Moscow, Russia

Received 31 October 2003

Published online 9 April 2004 – © EDP Sciences, Società Italiana di Fisica, Springer-Verlag 2004

Abstract. Magneto-optical properties of the materials with periodically modulated dielectric constant – photonic crystals (or band-gap materials) have been examined with relation to their possible applications for the control of electromagnetic radiation in the integrated optics devices. For this investigation we propose the original theoretical approach based on the perturbation theory. Magneto-optical Faraday and Voigt effects have been studied near extremum points of photonic bands where their significant enhancement takes place. On the grounds of the elaborated theory some experimental results are discussed. Experimentally obtained Faraday rotation angle frequency dependence shows good agreement with our theoretical predictions.

PACS. 78.20.Ls Magneto-optical effects – 78.20.Bh Theory, models, and numerical simulation – 73.21.Cd Superlattices

1 Introduction

Recently, there has been much attention paid to a new kind of dielectric composites – photonic crystals (PhC). Photonic crystals (also called photonic bandgap materials) are micro-structured materials in which the dielectric constant is periodically modulated on a length scale comparable to the desired wavelength of the electromagnetic radiation [1–3]. Multiple interferences between electromagnetic waves scattered from each unit cell results in a range of frequencies that do not propagate in the structure – photonic band gaps (PBG's). At these frequencies, the light is strongly reflected from the surface of the crystal, while at other frequencies light is transmitted. This phenomenon is of great theoretical and practical significance [4]. It can be used to study a wide range of physical problems related to the light localization [5] and light emission [6]. Photonic crystal materials with PBG's permit the fabrication of micro-cavity lasers [7], single mode light emitting diodes, highly efficient wave guides [8], high speed optical switches. However, PhC's, even those without a PBG, possess many other interesting properties related to the dispersion, anisotropy, and polarization characteristics of the photonic bands (PB). For example, these properties of PhC's offer the opportunity to create efficient dispersion compensation [9], enhanced nonlinear frequency conversion [10,11], novel superprism devices [12], optical polarizers, optical filters, and so on.

The tunability of PhC's optical properties can open new applications of these materials in the integrated optics devices. Tunability in semiconductor structures may be achieved by varying temperature [13] or by varying voltage [14]. Other ways of achieving tunability are application of elastic stress [15], liquid crystal infiltration [16], application of external magnetic fields or using magnetic constituents [17–26]. The latter two possibilities are of prime interest because they not only permit significant tunability but also can lead to some new interesting phenomena of magneto-optics such as enhanced magnetic circular and linear birefringence [23–26], mode conversion – phenomena which are essential for the novel readout devices and some devices of optical microcircuits.

In this paper, we will study magneto-optical effects of two dimensional PhC's composed either of dielectric or magnetic materials that implies a study of the magnetic field influence on the electromagnetic waves propagation in PhC's.

2 Basic equations and eigenvalues problem for magneto-optical medium

Let us consider dielectric nonuniform medium that is characterized by the dielectric constant $\varepsilon_{ij}(\vec{r}) = \delta_{ij}\varepsilon(\vec{r})$. Function $\varepsilon(\vec{r})$ is a periodic function $\varepsilon(\vec{r} + \vec{a}) = \varepsilon(\vec{r})$, where $\vec{a} = \{a_1\vec{e}_x + a_2\vec{e}_y\}$ – unit vector of the two dimensional (2D) PhC. We examine a physical system that consists of a periodic array of infinitely long, parallel, dielectric

^a e-mail: bvi@nm.ru

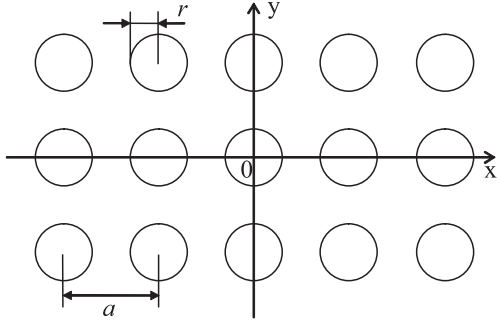


Fig. 1. Structure of two dimensional photonic crystal.

rods of dielectric constant ε_1 , embedded in a background dielectric material of dielectric constant ε_2 . The intersections of the rods axes with XY plane form a 2D periodic structure with square cell (Fig. 1).

The influence of magnetic field is taken into account by means of a polarization vector

$$\vec{P}_m(\vec{r}) = i\varepsilon_0\varepsilon(\vec{r})Q(\vec{r}) \cdot \vec{m} \times \vec{E} \quad (1)$$

where $\varepsilon_0 = 8.85 \times 10^{-12}$ F/m, \vec{m} – unit vector of magnetic field (or magnetization), $Q(\vec{r})$ – magneto-optical parameter, or Voigt parameter, of the medium (see e.g. [27]). For ferromagnetic substances Q is of the order of $10^{-3} \div 10^{-4}$: for yttrium iron garnets $Q = 0.5 \times 10^{-3}$ ($\lambda = 1.15$ mkm), and for bismuth-gadolinium iron garnets $Q = 26 \times 10^{-3}$ ($\lambda = 0.54$ mkm) [27]. For non-magnetic substances it is proportional to the external magnetic field \vec{B}_{ext} : for Si $Q = 1.2 \times 10^{-6}$ ($\lambda = 0.41$ mkm, $B_{ext} = 0.1$ T) [28], for europium glass $Q = 7 \times 10^{-5}$ ($\lambda = 0.435$ mkm, $B_{ext} = 0.1$ T) [29].

Assuming $\mu = 1$ it is straightforward to obtain from Maxwell's equations the following wave equation for $\vec{E}(\vec{r}, t)$:

$$\nabla \times \left\{ \nabla \times \vec{E}(\vec{r}, t) \right\} = -\frac{\partial^2}{\partial t^2} \left\{ \frac{\varepsilon(\vec{r})}{c^2} \vec{E}(\vec{r}, t) + \mu_0 \vec{P}_m(\vec{r}, t) \right\}, \quad (2)$$

where $\mu_0 = 4\pi \times 10^{-7}$ Vb/m², $c = (\varepsilon_0\mu_0)^{-1/2}$.

We seek the solution of (2) in the form $\vec{E}(\vec{r}, t) = \vec{E}(\vec{r})e^{-i\omega t}$, where ω is the eigen-angular frequency, and $\vec{E}(\vec{r})$ is eigenfunction of the wave equation (2). These eigenfunctions should thus satisfy the next eigenvalue equation:

$$L_E \vec{E}(\vec{r}) = \frac{1}{\varepsilon(\vec{r})} \nabla \times \left\{ \nabla \times \vec{E}(\vec{r}) \right\} - \left(\frac{\omega}{c} \right)^2 \vec{E}(\vec{r}) = \frac{\omega^2}{c^2 \varepsilon_0 \varepsilon(\vec{r})} \vec{P}_m(\vec{r}). \quad (3)$$

Linear operator \hat{L}_E defined by (3) is not a Hermitian operator. To pass to the Hermitian operator we, following [29], introduce a complex vectorial function $\vec{\Psi}(\vec{r}) = \sqrt{\varepsilon(\vec{r})} \vec{E}(\vec{r})$,

that leads to the eigenvalue equation:

$$\left(\hat{H} + \hat{V} - \frac{\omega^2}{c^2} \right) \vec{\Psi}(\vec{r}) = 0, \quad (4)$$

where

$$\hat{H} \vec{\Psi}(\vec{r}) = \frac{1}{\sqrt{\varepsilon(\vec{r})}} \nabla \times \left\{ \nabla \times \frac{1}{\sqrt{\varepsilon(\vec{r})}} \vec{\Psi}(\vec{r}) \right\}, \quad (5)$$

$$\hat{V} \vec{\Psi}(\vec{r}) = -i \left(\frac{\omega}{c} \right)^2 Q \cdot \vec{m} \times \vec{\Psi}(\vec{r}). \quad (6)$$

Operator \hat{H} has been studied rigorously elsewhere [30,31]. Eigenfunctions of \hat{H} are vectorial Bloch functions

$$\vec{\Psi}_{n\vec{k}}(\vec{r}) = \vec{u}_{n\vec{k}}(\vec{r}) e^{i\vec{k}\vec{r}}, \quad (7)$$

where \vec{k} is quasi-momentum and n is a number of the given PB; $u_{n\vec{k}}(\vec{r}_{||}) = u_{n\vec{k}}(\vec{r}_{||} + \vec{a})$, $\vec{r}_{||} = x\vec{e}_x + y\vec{e}_y$. Corresponding eigenvalues ω_n form a band diagram with alternating permitted bands and bandgaps. We will assume as usual that vector \vec{k} belongs to the first Brillouin zone. These properties of eigenfunctions and eigenvalues are well-known in the crystal physics and are direct consequences of operator's \hat{H} periodicity.

Operator \hat{V} describes interaction of electromagnetic radiation with magnetic part of the medium's polarization. It is proportional to the magneto-optical parameter that is much smaller than 1. Consequently, operator \hat{V} can be treated on the ground of perturbation theory.

Substitution of (7) into (4) gives

$$\left(\hat{H} + \hat{V} - \frac{\omega^2}{c^2} \right) \vec{u}_{n\vec{k}} = 0, \quad (8)$$

where

$$\hat{H} \vec{u}_{n\vec{k}} = \frac{1}{\sqrt{\varepsilon}} \nabla \times \nabla \times \frac{\vec{u}_{n\vec{k}}}{\sqrt{\varepsilon}} + \frac{i\vec{k}}{\sqrt{\varepsilon}} \times \nabla \times \frac{\vec{u}_{n\vec{k}}}{\sqrt{\varepsilon}} + \frac{i}{\sqrt{\varepsilon}} \nabla \times \vec{k} \times \frac{\vec{u}_{n\vec{k}}}{\sqrt{\varepsilon}} - \frac{\vec{k}}{\varepsilon} \times \vec{k} \times \vec{u}_{n\vec{k}}, \quad (9)$$

$$\hat{V} \vec{u}_{n\vec{k}} = -i \frac{\omega^2}{c^2} Q(\vec{r}_{||}) \cdot \vec{m} \times \vec{u}_{n\vec{k}}. \quad (10)$$

3 Eigenfunctions and their symmetry for the nonmagnetic case

3.1 Two types of operator \hat{H} modes

One of the main features of operator \hat{H} is that its eigenfunctions can be divided into two types: quasi-longitudinal modes $\vec{\Psi}_{n\vec{k}}^{(L)}(\vec{r})$ and quasi-transverse $\vec{\Psi}_{n\vec{k}}^{(T)}(\vec{r})$ modes. The former are given by [30]

$$\vec{\Psi}_{n\vec{k}}^{(L)}(\vec{r}) = C \sqrt{\varepsilon(\vec{r})} \frac{\vec{k} + \vec{G}_n}{|\vec{k} + \vec{G}_n|} \exp \left\{ i \left(\vec{k} + \vec{G}_n \right) \vec{r} \right\}, \quad (11)$$

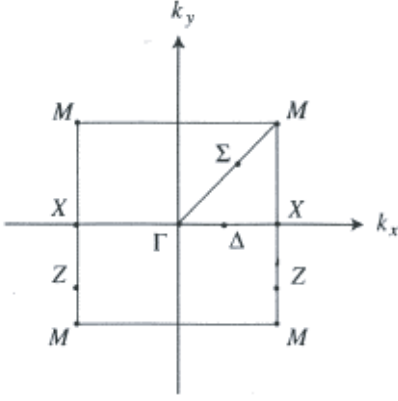


Fig. 2. The first Brillouin zone for two dimensions.

where \vec{G}_n is a reciprocal lattice vector and C is a normalization constant. It can be shown easily that $\vec{\Psi}_{n\vec{k}}^{(L)}(\vec{r})$ satisfies

$$\nabla \times \left\{ \frac{1}{\sqrt{\varepsilon(\vec{r})}} \vec{\Psi}_{n\vec{k}}^{(L)}(\vec{r}) \right\} = 0, \quad (12)$$

that gives $\hat{H} \vec{\Psi}_{n\vec{k}}^{(L)}(\vec{r}) = 0$. This equation implies that $\vec{\Psi}_{n\vec{k}}^{(L)}(\vec{r})$ is an eigenfunction of \hat{H} with eigen-angular frequency $\omega_{n\vec{k}}^{(L)} = 0$. At the same time, $\vec{\Psi}_{n\vec{k}}^{(L)}(\vec{r})$ modes do not satisfy Maxwell's divergence equation, i.e. $\nabla \cdot \left\{ \sqrt{\varepsilon(\vec{r})} \vec{\Psi}_{n\vec{k}}^{(L)}(\vec{r}) \right\} \neq 0$, and, consequently, they are not existent. However, these modes are essential mathematically, since without them eigenfunctions system $\vec{\Psi}_{n\vec{k}}^{(L)}(\vec{r})$ is not complete.

Transversal eigenfunctions $\vec{\Psi}_{n\vec{k}}^{(T)}(\vec{r})$ satisfy

$$\hat{H} \vec{\Psi}_{n\vec{k}}^{(T)}(\vec{r}) = \left(\frac{\omega_{n\vec{k}}^{(T)}}{c} \right)^2 \vec{\Psi}_{n\vec{k}}^{(T)}(\vec{r}) \quad (13)$$

with eigen-angular frequencies $\omega_{n\vec{k}}^{(T)}$ that are generally non-zero. These modes satisfy Maxwell's divergence equation and do really exist.

Eigenfunctions $\vec{\Psi}_{n\vec{k}}^{(T)}(\vec{r})$ form a complete set in the Hilbert space. They are not orthogonal to each other but can be orthogonalized by e.g. Schmidt's method.

3.2 Symmetry of eigenfunctions

In this paper we restrict our analysis to the consideration of highly symmetrical points in the first Brillouin zone (points Γ , X , et al., see Fig. 2) in which properties of light propagation differ substantially from those for uniform media.

Two dimensional PhC apart from the translational symmetry can possess several other spatial symmetries such as rotational symmetries **2**, **3**, **4**, **6**, mirror reflection invariance, inversion symmetry.

Together with the identity operation **1** that keeps the structure as it is, these symmetry operations constitute the G point group of the PhC. It means that for any operation R from the G point group ($\forall R \in G$) $R\varepsilon(\vec{r}) = \varepsilon(\vec{r})$, that is, PhC is invariant with respect to the operations of group G .

The symmetry of the eigenfunctions of the PhC's is very important for understanding their optical and magneto-optical properties (for details see [30]).

Point group for 2D PhC with square lattice represents

$$4mm = \{ \mathbf{1}, \mathbf{2}, \mathbf{4}, \bar{\mathbf{4}}, m_x, m_y, m_d, m'_d \}, \quad (14)$$

where **2**, **4**, $\bar{\mathbf{4}}$ are rotations by π , $\frac{\pi}{2}$, $-\frac{\pi}{2}$ about Z -axis, respectively; m_x , m_y , m_d , m'_d are mirror reflections in the planes that contain Z -axis and Y -axis, X -axis, quadrant diagonals $y = x$, $y = -x$, respectively.

Operators of the G point group also transform vectors \vec{k} from the first Brillouin zone. Any vector \vec{k} is characterized by its own $G_{\vec{k}}$ group which is the subgroup of the G group. Groups of the some highly symmetrical points in the first Brillouin zone are more substantial. For 2D PhC's with the $4mm$ point group there are several subgroups:

$$\begin{aligned} G_{\Gamma} &= G_M = 4mm, \\ G_X &= \{ \mathbf{1}, \mathbf{2}, m_x, m_y \} = 2mm, \\ G_{\Delta} &= \{ \mathbf{1}, m_y \} = 1m, \\ G_{\Sigma} &= \{ \mathbf{1}, m_d \} = 1m, \\ G_Z &= \{ \mathbf{1}, m_x \} = 1m. \end{aligned} \quad (15)$$

It is known from the crystals band theory that classification of eigenfunctions of operator \hat{H} can be represented on the basis of irreducible representations $G_{\vec{k}}$ groups. Tables 1a and b are character tables for $4mm$ and $2mm$ points groups. In these tables A_1, A_2, B_1, B_2 are one-dimensional irreducible representations and E is two-dimensional irreducible representation. Here, "one-dimensional" means that the eigenmode is not degenerate and "two-dimensional" means that the eigenmode is doubly degenerate. The existence of two dimensional modes is possible only at Γ and M points of the first Brillouin zone.

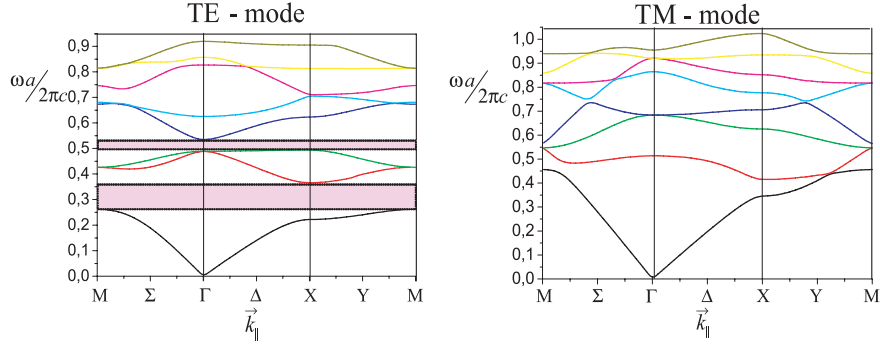
Mirror reflection operations are particularly of great importance. Their presence in some $G_{\vec{k}}$ groups permits the division of the eigenmodes into two types that differ in the parity with respect to the reflection in the given plane: even (A) and odd (B) modes. This fact is significant for the establishment of the selection rules for transmittance and reflection from PhC's, for some nonlinear processes, for the elimination of the unphysical solutions *et al.* It is used below for the calculation of matrix elements of operator \hat{V} .

For 2D PhC symmetry $z \rightarrow -z$ enables to classify all eigenmodes into two kinds: TE modes (E_z, H_x, H_y) and TM modes (E_x, E_y, H_z). Each of them, as was mentioned above, is characterized by additional parity with respect to the reflection in the corresponding vertical planes.

Table 1. Character table for the 4 mm (a) and 2 mm (b) point groups.

4 mm	1	4	2	m_x	m_d
A_1	1	1	1	1	1
A_2	1	1	1	-1	-1
B_1	1	-1	1	1	-1
B_2	1	-1	1	-1	1
E	2	0	-2	0	0

2 mm	1	2	m_x	m_y
A_1	1	1	1	1
A_2	1	1	-1	-1
B_1	1	-1	-1	1
B_2	1	-1	1	-1

**Fig. 3.** Photonic band structure of TE and TM-modes in 2D PhC made of air rods in Si-material ($\epsilon_1 = 1$, $\epsilon_2 = 11.7$). Filling factor of the rods is 0.785. The second bandgap occurs for normalized angular frequencies from 0.492 to 0.537. It corresponds to the range of wavelengths in vacuum from 745 nm to 813 nm for PhC lattice constant $a = 0.4$ mkm.

4 Perturbation theory approach

To remove an ambiguity, in this paper we restrict our consideration to Γ and X extremum points in the first Brillouin zone and assume that wave packet in PhC is constituted by Bloch functions $\vec{\Psi}_{n\vec{k}}(\vec{r})$ from one or two PB's (depending on the concrete situation) with \vec{k} lying in the vicinity of the critical point. This assumption is similar to the adiabatic approximation in the solid state physics and is applicable to the sufficiently small value of perturbation \hat{V} . Thus, quasi-momentum $\vec{k} = (k_0 + \kappa, 0, 0)$, where $k_0 = 0$ for Γ point and $k_0 = \frac{\pi}{a}$ for τ point, $\kappa \ll k_0$.

Operator \hat{H} in (8) can be presented as the sum of \hat{H}_0 and \hat{H}_1 operators:

$$\hat{H} = \hat{H}_0 + \hat{H}_1, \quad (16)$$

where

$$\hat{H}_0 \vec{u}_{n\vec{k}} = \frac{1}{\sqrt{\epsilon}} \nabla \times \nabla \times \frac{\vec{u}_{n\vec{k}}}{\sqrt{\epsilon}} + k_0 \hat{\partial}_1 \frac{\vec{u}_{n\vec{k}}}{\sqrt{\epsilon}} + \frac{k_0^2}{\epsilon} \vec{u}_{n\vec{k}}, \quad (17)$$

$$H_1 \vec{u}_{n\vec{k}} = \kappa \hat{\partial}_2 \frac{\vec{u}_{n\vec{k}}}{\sqrt{\epsilon}} + \frac{2k_0 \kappa}{\epsilon} \vec{u}_{n\vec{k}} + \frac{\kappa^2}{\epsilon} \vec{u}_{n\vec{k}}, \quad (18)$$

$\hat{\partial}_1, \hat{\partial}_2$ -operators that consist of the first spatial partial derivatives.

For k close to k_0 (i.e. $\kappa \ll k_0$) operator \hat{H}_1 , along with \hat{V} , are perturbations. In the zeroth order on κ and Q the solutions of (8) are Bloch functions for different wave zones. Eigenfunctions of $\hat{H}_0 - \vec{u}_{nk_0}(\vec{r}_{||})$ form complete basis for the expansion of any function that possesses translational symmetry. Hence, we can refer to them as

a basis for the expansion of any eigenfunction $\vec{u}_{n_0 k}(\vec{r}_{||})$ of operator \hat{H} into series in perturbation theory. Eigenangular frequencies of $\hat{H}_0 - \omega_{n_0}$ is to be found by means of solving eigenvalues problem for the set of linear equations obtained from Maxwell's equations. There are several algorithms for it. In our calculations we used a procedure that was proposed in [31]. Examples of PB's structures are presented in Figure 3.

Dispersion function $\omega = \omega(k)$ has extremums at the critical points of the Brillouin zone and, consequently, does not contain terms proportional to the first power of κ . Therefore, in operator \hat{H}_1 , defined by (18), one can omit terms with κ and operator \hat{H}_1 is given by $H_1 \vec{u}_{n\vec{k}} = \frac{\kappa^2}{\epsilon} \vec{u}_{n\vec{k}}$.

5 Magneto-optics of photonic crystals

5.1 Faraday geometry

There are two main geometries in magneto-optics: (i) longitudinal, or Faraday, geometry when electromagnetic wave propagates along magnetic field, i.e. $\vec{k} || \vec{m}$, (ii) transversal, or Voigt, geometry when $\vec{k} \perp \vec{m}$.

Let us first consider longitudinal geometry for which $\vec{k} || \vec{m} || \vec{e}_x$ and investigate how the presence of magnetic field affects PB of arbitrary number n_0 . Here several cases are possible: (i) n_0 th PB is not degenerate and single, (ii) n_0 th PB is not degenerate, but has close neighbor PB, (iii) n_0 -th PB is doubly degenerate (possible only at Γ and M points). The meaning of the word "close" in (ii) will be discussed further (see Sect. 5.1.2). We examine two first possibilities in turn.

5.1.1 The case of single wave zone

Function $\vec{u}_{n_0k}(\vec{r}_{||})$, that represents the eigenfunction of (8) for n_0 th PB, can be written in the first order of perturbation theory as

$$\vec{u}_{n_0k}(\vec{r}_{||}) = c_1 u_{n_0k_0}^{TE}(\vec{r}_{||}) \vec{e}_z + c_2 u_{n_0k_0}^{TM}(\vec{r}_{||}) \vec{e}_y + c_3 u_{n_0k_0}^L(\vec{r}_{||}) \vec{e}_x, \quad (19)$$

where $u_{n_0k_0}^{TE}$, $u_{n_0k_0}^{TM}$, and $u_{n_0k_0}^L$ are eigenfunctions of operator \hat{H}_0 :

$$\hat{H}_0 u_{n_0k_0}^{TE(TM)} = \frac{(\omega_{n_0}^{TE(TM)})^2}{c^2} u_{n_0k_0}^{TE(TM)}; \quad \hat{H}_0 u_{n_0k_0}^L = 0. \quad (20)$$

In Faraday geometry $c_3 = 0$ because $\hat{V} u_{n_0k_0}^L = 0$. Eigenfunctions $u_{n_0k_0}^{TE}$ and $u_{n_0k_0}^{TM}$ usually have different parity.

Substitution of (19) in (8) leads to the following equations set:

$$\begin{cases} c_1 \{(\omega_{n_0k}^{TE})^2 - \omega^2\} - c_2 i \omega^2 \langle Q \rangle = 0 \\ c_2 \{(\omega_{n_0k}^{TM})^2 - \omega^2\} + c_1 i \omega^2 \langle Q \rangle^* = 0 \end{cases}, \quad (21)$$

where

$$(\omega_{n_0k}^{TE(TM)})^2 = (\omega_{n_0}^{TE(TM)})^2 + c^2 \kappa^2 \beta^{TE(TM)}, \quad (22)$$

$$\beta^{TE(TM)} = \left\langle u_{n_0k_0}^{TE(TM)} \left| \frac{1}{\varepsilon(\vec{r}_{||})} \right| u_{n_0k_0}^{TE(TM)} \right\rangle \quad (23)$$

$$\langle Q \rangle = \left\langle u_{n_0k_0}^{TE} \left| Q(\vec{r}_{||}) \right| u_{n_0k_0}^{TM} \right\rangle. \quad (24)$$

In the next order of perturbation theory general structure of (21) is preserved but coefficients $\beta^{TE(TM)}$ and $\langle Q \rangle$ are renormalized. Thus, for $\beta^{TE(TM)}$ we have:

$$\begin{aligned} \beta^{TE(TM)} &= \left\langle u_{n_0k_0}^{TE(TM)} \left| \frac{1}{\varepsilon(\vec{r}_{||})} \right| u_{n_0k_0}^{TE(TM)} \right\rangle \\ &+ \kappa^2 c^2 \sum_{n \neq n_0} \frac{\left| \left\langle u_{nk_0}^{TE(TM)} \left| \frac{1}{\varepsilon(\vec{r}_{||})} \right| u_{n_0k_0}^{TE(TM)} \right\rangle \right|^2}{(\omega_{n_0}^{TE(TM)})^2 - (\omega_n^{TE(TM)})^2}. \end{aligned} \quad (25)$$

Parameter $\langle Q \rangle$ is renormalized in the same manner. We should notice here that in (25) the summation is to be taken on PB's with the same parity as n_0 th PB. On the contrary, in the corresponding expression for $\langle Q \rangle$ one should summate only PB's with opposite parities (see Sect. 3).

It follows from (21) that

$$\{(\omega_{n_0k}^{TE})^2 - \omega^2\} \{(\omega_{n_0k}^{TM})^2 - \omega^2\} - \omega^4 |\langle Q \rangle|^2 = 0. \quad (26)$$

For revelation of the general features of the magneto-optical effects in the given geometry we assume that

$$\omega_{n_0}^{TE} = \omega_{n_0}^{TM} \equiv \omega_{n_0} \quad \text{and} \quad \beta^{TE} = \beta^{TM} \equiv \beta. \quad (27)$$

This supposition is adequate for 3D PhC for singlet PB near Γ point.

On these assumptions equation (26) leads to the following solutions for κ :

$$\kappa_{\pm} = \frac{\omega}{c\sqrt{|\beta|}} \left(\left| 1 - \frac{(\omega_{n_0})^2}{(\omega)^2} \pm |\langle Q \rangle| \right| \right)^{1/2}, \quad (28)$$

and corresponding eigenfunctions:

$$\vec{\psi}^{\pm}(\vec{r}_{||}) = \begin{pmatrix} u_{n_0k_0}^{TE}(\vec{r}_{||}) \\ \mp i u_{n_0k_0}^{TM}(\vec{r}_{||}) \end{pmatrix} e^{i(k_0 + \kappa_{\pm})x}. \quad (29)$$

These eigenmodes can be called ‘‘quasi-circularly polarized’’ modes. Prefix ‘‘quasi’’ here means that waves $\vec{\psi}^{\pm}(\vec{r}_{||})$ in (29) are the product of fast oscillating functions $u_{n_0k_0}^{TE(TM)}(\vec{r}_{||})$ and comparatively slow changing envelope functions $e^{i(k_0 + \kappa_{\pm})x}$. If at $x = 0$ $\vec{\psi}(\vec{r}_{||}) = \begin{pmatrix} u_{n_0k_0}^{TE} \\ 0 \end{pmatrix}$, then

$$\vec{\Psi}(\vec{r}_{||}) = e^{ik_0x} e^{i\frac{\kappa_+ + \kappa_-}{2}x} \begin{pmatrix} u_{n_0k_0}^{TE}(x) \cos \frac{\Delta\kappa}{2}x \\ u_{n_0k_0}^{TM}(x) \sin \frac{\Delta\kappa}{2}x \end{pmatrix}, \quad (30)$$

where $\Delta\kappa = \kappa_+ - \kappa_-$. Equation (30) shows that while light propagates along OX-axis mode conversion takes place. If at the PhC's entry electromagnetic radiation is TE-wave then while spreading it transforms into TM-wave because of the medium gyrotropy and so on. Usually, condition

$$|\langle Q \rangle| \ll \left| 1 - \frac{(\omega_{n_0})^2}{(\omega)^2} \right| \quad (31)$$

is satisfied and specific Faraday angle or rotation angle of envelope wave's polarization plane per unit length is

$$\Phi = \frac{\Delta\kappa}{2} = \frac{\kappa_+ - \kappa_-}{2} = \frac{\omega}{2c\sqrt{|\beta|}} |\langle Q \rangle| \left| 1 - \frac{(\omega_{n_0})^2}{(\omega)^2} \right|^{-1/2}. \quad (32)$$

From (32) one can infer that specific Faraday angle grows sharply when $\omega \rightarrow \omega_{n_0}$. It happens in compliance with fundamental property of PhC's: near extremum points of Brillouin zone critical deceleration of radiation takes place that leads to the increase in the interaction time between radiational mode and the matter system and, thus, magneto-optical effect is enhanced.

It is interesting to compare obtained result with the experimental measure of Faraday rotation angle for 3D magnetic colloidal crystal consisting of a fcc packing of silica spheres with voids that are filled with a saturated glycerol solution of dysprosium nitrate [32]. Though formula (32) was obtained for the 2D-PhC one can expect that it is valid for some cases in 3D. For example, the propriety of its application at Γ point for cubic 3D PhC becomes intuitively clear when we conduct the analogue with the electron zones of some semiconductors (e.g. GaAs). Continuing this analogue one can conclude that conditions (27) are met there and (32) remains valid. Approximation of experimental curves with the theoretical dependence is quite

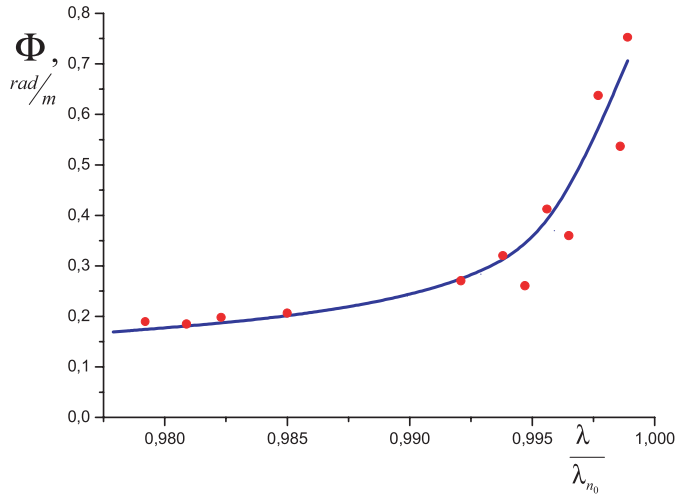


Fig. 4. Faraday rotation angle versus $\frac{\lambda}{\lambda_{n_0}}$. Points-experiment data for 3D magnetic colloidal crystal consisting of a fcc packing of silica spheres with voids that are filled with a saturated glycerol solution of dysprosium nitrate ($d_{spheres} = 260$ nm, $\varepsilon_{silica} = 2.0$, $\varepsilon_{liquid} = 2.2$, $B_{ext} = 33.5$ mT, $Q = 1 \times 10^7$) [32]. Solid curve – theory (in accordance to (32)), $\lambda_{n_0} = 566.5$ nm.

good that confirms our assumption (Fig. 4). At this approximation the ratio $\frac{|Q|}{\sqrt{|\beta|}}$ plays role of the fitting parameter. For the curve in Figure 4 $\frac{|Q|}{\sqrt{|\beta|}} = 6.55 \times 10^{-9}$.

When ω becomes very close to ω_{n_0} then (31) is no longer satisfied and for determination of the specific Faraday rotation one should use (28) directly without any approximations. More careful analysis of $\Phi(\omega)$ dependence reveals that it has extremum for $\omega = \omega_{n_0}(1 \pm 1/2Q)$ (choice between “+” and “-” here depends on the sign of β , i.e. on the sign of the second derivative of PB’s dispersion curve). This formula is very important because it shows that Faraday effect takes maximum value not exactly at the extremum angular frequency ω_{n_0} , for which transmission is negligibly small, but at its close proximity where transmission is higher. Maximum value of specific Faraday rotation is given by

$$\Phi = \frac{\omega_{n_0}}{c\sqrt{|\beta|}} \sqrt{\frac{|Q|}{2}}. \quad (33)$$

At the same time Faraday rotation for the uniform media is

$$\Phi_{uniform} = \frac{\omega}{2c} \sqrt{\varepsilon} Q. \quad (34)$$

From (33) and (34) taking into account (23) and (24) one can estimate relative gain of Faraday effect in PhC in comparison to the same uniform medium under the same conditions:

$$\frac{\Phi_{PhC}}{\Phi_{uniform}} \sim \sqrt{\frac{1}{Q}}. \quad (35)$$

Thus for $Q = 10^{-6}$ Faraday effect in PhC can be enhanced by three orders.

We define conversion coefficient R as the ratio of the maximum squared amplitudes of the TE- and TM-modes

if at $x = 0$ TM-wave is supposed to exist. For the conditions (27) $R \sim 1$.

For different and not very close $\left(|Q| \ll \left| \frac{(\omega_{n_0}^{TE})^2 - (\omega_{n_0}^{TM})^2}{(\omega)^2} \right| \right)$ $\omega_{n_0}^{TE}$ and $\omega_{n_0}^{TM}$, but with condition $\beta^{TE} = \beta^{TM} \equiv \beta$, eigenfunctions equal

$$\begin{aligned} \vec{\psi}^{\pm}(\vec{r}_{||}) = c_1 & \left(i\xi u_{n_0 k_0}^{TE}(\vec{r}_{||}) \right) e^{i(k_0 + \kappa_+)x} \\ & + c_2 \left(-\frac{i}{\xi} u_{n_0 k_0}^{TE}(\vec{r}_{||}) \right) e^{i(k_0 + \kappa_-)x}, \quad (36) \\ & + c_1 \left(u_{n_0 k_0}^{TM}(\vec{r}_{||}) \right) e^{i(k_0 + \kappa_+)x} \\ & + c_2 \left(u_{n_0 k_0}^{TM}(\vec{r}_{||}) \right) e^{i(k_0 + \kappa_-)x}, \end{aligned}$$

where $\xi = \frac{\omega^2 |Q|}{(\omega_{n_0}^{TE})^2 - (\omega_{n_0}^{TM})^2}$. For this case effect of birefringence appears, conversion coefficient R decreases and is of the order of ξ^2 as in birefringent crystals (see for example [27]). If electromagnetic radiation is linear polarized at the entrance of PhC then while spreading in PhC polarization mainly preserves with very little ellipticity. At the same time, TE-TM modes partial conversion takes place at much smaller distances.

Distinction between values of β^{TE} and β^{TM} complicates analysis. For some values of $\frac{\omega_{n_0}^{TE}}{\omega_{n_0}^{TM}}$ TE - mode prevails and for other values – TM-mode prevails for arbitrary entry polarization.

General impact of magnetic field on PB structure is expressed in the contraction of PBG’s: PB’s in magnetic field shift at $Q\omega_{n_0}$.

For magneto-optical parameter $Q = 5 \times 10^{-3}$ the shift is about several tenths of percent. The value of the shift depends on the difference $\omega_{n_0}^{TE} - \omega_{n_0}^{TM}$ and gets smaller when the difference increases.

5.2 The case of two close wave zones

The situation when two PB’s are close exists quite often and undoubtedly deserves special examination. We consider two consecutive zones of numbers n_0 and $n_0 + 1$ with corresponding frequencies $\omega_0^{TE(TM)} - \Delta^{TE(TM)}$ and $\omega_0^{TE(TM)} + \Delta^{TE(TM)}$ for TE- and TM-modes, where $\omega_0^{TE(TM)}$ is the middle frequency and $\Delta^{TE(TM)}$ is the half-width of the PBG between given zones (Fig. 5). To begin, let us define what “close” means at this point. The singlet PB’s splitting that arises in magnetic field is of the order of $\omega_{n_0} Q$ (it follows from (28)). That is why we call two wave zones “close” if the distance between them smaller than this magnetic caused splitting, i.e. $2\Delta < \omega_{n_0} Q$.

At Γ and X points parities of two consecutive bands are usually opposite, so for the sake of distinctness we assume that TE-eigenfunction for n_0 th band has parity of B_1 and for $(n_0 + 1)$ th band – parity of A_1 (see Tabs. 1 a and b) and vice versa for TM-eigenfunctions.

Function $\vec{u}_{n_0 k}(\vec{r}_{||})$, that represents the eigenfunction of (8) for two close PB’s for magnetic case, can be written

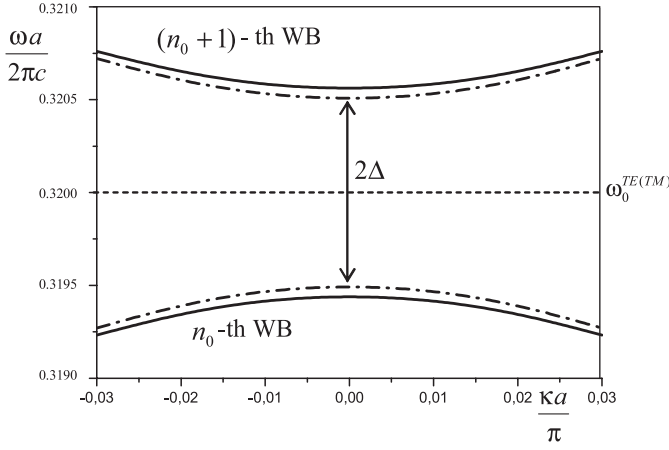


Fig. 5. Two close photonic bands of numbers n and $n + 1$ at the vicinity of X point in the Brillouin zone. Distance between bands at X point is Δ . (it is assumed that for TE- and TM-modes interband distances and extremum angular frequencies are the same: $\omega_0^{TE} = \omega_0^{TM} \equiv \omega_0$, $\Delta^{TE} = \Delta^{TM} = \Delta$).

in the first order of perturbation theory as

$$\vec{u}_{n_0 k}(\vec{r}_{||}) = \left(c_1 u_{n_0 k_0}^{TE}(\vec{r}_{||}) + c_2 u_{(n_0+1), k_0}^{TE}(\vec{r}_{||}) \right) \vec{e}_z + \left(c_3 u_{n_0 k_0}^{TM}(\vec{r}_{||}) + c_4 u_{(n_0+1), k_0}^{TM}(\vec{r}_{||}) \right) \vec{e}_y. \quad (37)$$

Procedure similar to the one in 5.1.1 gives the following equations set for coefficients c_i :

$$\begin{cases} c_1 ((\omega_1^{TE})^2 - \omega^2) - c_4 i \omega^2 \langle Q_B \rangle = 0 \\ c_4 ((\omega_2^{TM})^2 - \omega^2) + c_1 i \omega^2 \langle Q_B \rangle^* = 0 \\ c_2 ((\omega_2^{TE})^2 - \omega^2) - c_3 i \omega^2 \langle Q_A \rangle = 0 \\ c_3 ((\omega_1^{TM})^2 - \omega^2) + c_2 i \omega^2 \langle Q_A \rangle^* = 0 \end{cases}, \quad (38)$$

where

$$\begin{aligned} \left(\omega_i^{TE(TM)} \right)^2 &= \\ \begin{cases} \left(\omega_0^{TE(TM)} - \Delta^{TE(TM)} \right)^2 + \kappa^2 c^2 \beta_1^{TE(TM)}, i = 1 \\ \left(\omega_0^{TE(TM)} + \Delta^{TE(TM)} \right)^2 + \kappa^2 c^2 \beta_2^{TE(TM)}, i = 2 \end{cases}, \\ \beta_i^{TE(TM)} &= \left\langle u_{(n_0-1+i), k_0}^{TE(TM)} \left| \frac{1}{\varepsilon} \right| u_{(n_0-1+i), k_0}^{TE(TM)} \right\rangle, \\ i = 1, 2, \langle Q_A \rangle &= \left\langle u_{(n_0+1), k_0}^{TE} \left| Q(\vec{r}_{||}) \right| u_{n_0, k_0}^{TM} \right\rangle, \\ \langle Q_B \rangle &= \left\langle u_{n_0, k_0}^{TE} \left| Q(\vec{r}_{||}) \right| u_{(n_0+1), k_0}^{TM} \right\rangle. \end{aligned}$$

While derivation of (38) eigenfunctions symmetry properties were taken into consideration (see Sect. 3). Thus, it is evident from symmetry considerations that some matrix elements such as $\left\langle u_{(n_0+1), k_0}^{TE} \left| Q(\vec{r}_{||}) \right| u_{(n_0+1), k_0}^{TM} \right\rangle$, $\left\langle u_{n_0, k_0}^{TE} \left| \frac{1}{\varepsilon(\vec{r}_{||})} \right| u_{(n_0+1), k_0}^{TE} \right\rangle$ et al. vanish. From (38) a dispersion relation can be obtained. For the case when $\omega_0^{TE} =$

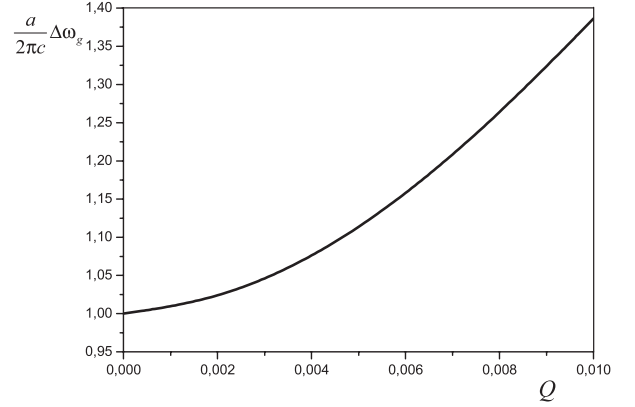


Fig. 6. Band gap width $\Delta\omega_g$ versus magneto-optical parameter Q ; $\omega_0^{TE} = \omega_0^{TM} \equiv \omega_0 = 0.32 \frac{2\pi c}{a}$, $\Delta^{TE} = \Delta^{TM} = 5 \times 10^{-4} \frac{2\pi c}{a}$.

$\omega_0^{TM} \equiv \omega_0$, $\Delta^{TE} = \Delta^{TM} = \Delta$ and $\beta_i^{TE} = \beta_i^{TM} \equiv \beta$ this dispersion relation takes simple form:

$$\kappa = \frac{\omega}{c\sqrt{|\beta|}} \left(\sqrt{\left(1 - \frac{\omega_0^2 + \Delta^2}{\omega^2} \right)^2 - Q^2 - 2 \frac{\omega_0 \Delta}{\omega^2}} \right)^{1/2}, \quad (39)$$

which implies that for any fixed frequency ω from n_0 th or $(n_0 + 1)$ th close PB's only one electromagnetic mode propagates and nor transformation exists. However, the presence of magnetic field influences on the PBG's width $\Delta\omega_g$:

$$\Delta\omega_g = \omega_0 \sqrt{\left(\frac{2\Delta}{\omega_0} \right)^2 + Q^2}, \quad (40)$$

making it larger (Fig. 6).

5.3 Voigt geometry. Magnetic birefringence

The other important configuration is the Voigt geometry when $\vec{B}_{ext} \parallel \vec{e}_z$ and $\vec{k} \parallel \vec{e}_x$. The analysis of this case can be done in the same manner as for Faraday geometry in Section 5.1.

5.3.1 The case of single wave zone

Eigenfunction $\vec{u}_{n_0 k}(\vec{r}_{||})$ of (8) for n_0 th PB, is again given by (19), but for the Voigt geometry coefficient c_3 in (19) no longer vanishes. Substitution of (19) in (8) leads to the two independent subsets: one for $u_{n_0 k_0}^{TE}$, and the other for $u_{n_0 k_0}^{TM}$ and $u_{n_0 k_0}^L$. The former subset gives wave vector for TE - mode:

$$\kappa_{||} = \frac{\omega}{c\sqrt{|\beta^{TE}|}} \left| 1 - \left(\frac{\omega_{n_0}^{TE}}{\omega} \right)^2 \right|^{1/2}. \quad (41)$$

The second subset leads to the following simultaneous equations:

$$\begin{cases} c_2 \{ (\omega_{n_0 k}^{TM})^2 - \omega^2 \} - c_3 i \omega^2 \langle Q_L \rangle^* = 0 \\ c_2 i \langle Q_L \rangle - c_3 = 0 \end{cases}, \quad (42)$$

where $\langle Q_L \rangle = \langle u_{n_0 k_0}^L | Q(\vec{r}_{||}) | u_{n_0 k_0}^{TM} \rangle$. This equations set has nontrivial solution when

$$\kappa_{\perp} = \frac{\omega}{c\sqrt{|\beta^{TM}|}} \left| 1 - \left(\frac{\omega_{n_0}^{TM}}{\omega} \right)^2 - |\langle Q_L \rangle|^2 \right|^{1/2}. \quad (43)$$

Comparing (41) and (43) one can determine relative phase shift between TE- and TM-modes at the unit length:

$$B_{mb} = \text{Re}(\kappa_{||} - \kappa_{\perp}) = \frac{\omega}{2c\sqrt{|\beta|}} |\langle Q_L \rangle|^2 \left| 1 - \frac{\omega_{n_0}^2}{\omega^2} \right|^{-1/2}, \quad (44)$$

we have assumed here that conditions (27) are satisfied and $|\langle Q_L \rangle| \ll \left| 1 - \frac{(\omega_{n_0})^2}{(\omega)^2} \right|$.

This effect of magnetic birefringence is analogous to the magneto-optical Voigt effect (see e.g. [27]). In comparison to the latter, formula (44) demonstrates sharp increase of the phase shift B_{mb} near the extremum points of Brillouin zone. It is largely due to the same reasons as the increase of Faraday rotation (see Sect. 5.1.1).

It is evident from (41) and (43) that presence of magnetic field affects only on TM-mode shifting its corresponding PB. The value of this shift is of the order of $\omega_{n_0} Q^2$ and, consequently, much smaller than in Faraday geometry.

5.3.2 The case of two close wave zones

Consideration of the case when the distance between two PB's is $2\Delta^{TE(TM)}$ and $\Delta^{TE(TM)} \leq \omega_0 Q^2$ (see Sect. 5.2.1) can be done in the similar manner as for the Faraday geometry (see Sect. 5.1.2).

Magnetic field influences only on TM – mode and, thus, only κ_{\perp} depends on Q_L :

$$\kappa_{\perp}^{\pm} = \frac{\omega}{c\sqrt{|\beta|}} \left(1 - \frac{\omega_0^2 + \Delta^2}{\omega^2} - Q_L^2 \pm \sqrt{4 \frac{(\omega_0 \Delta)^2}{\omega^4} + Q_L^4} \right)^{1/2}. \quad (45)$$

6 Conclusion

We have studied magneto-optical properties of two dimensional PhC's composed either of dielectric or magnetic materials that implies an investigation of the magnetic field influence on the electromagnetic waves propagation in PhC's. Theoretical investigation has been performed on the basis of solving eigenvalues problem obtained from Maxwell's equations. Magnetic part of the medium's polarization has been considered as a perturbation and corresponding magneto-optical effects were calculated in the first order of perturbation theory. Two main geometries have been examined: the Faraday and Voigt configurations.

In the Faraday geometry in which $\vec{k} || \vec{m} || \vec{e}_x$ the TE-TM mode conversion takes place – the effect similar to the magneto-optical Faraday effect. The Faraday angle depends on the wave frequency ω and increases sharply when ω approaches extremum frequencies ω_{n_0} of wave bands. However, Faraday effect takes its maximum value not exactly at ω_{n_0} , but at its close proximity (see Sect. 5.1.1) where transmission coefficient is not too small. Substantial increase in the Faraday effect happens for ferromagnetic constituents. Thus for the magnetic material with magneto-optical parameter $Q \sim 10^{-3}$ the Faraday rotation angle can be as large as $20^\circ/mkm$ for near infrared radiation. This phenomenon is very promising for construction of the miniature optical isolators in the integrated optics. Relative enhancement of the Faraday rotation in PhC with respect to the uniform medium is larger for smaller values of Q (see Sect. (35)). That makes applications of nonmagnetic substances with magnetic field induced gyrotropy (for which $Q \sim 10^{-5} - 10^{-7}$) for the fabrication of PhC's the most valuable.

Comparison of the theoretical formula for Faraday rotation with experimental data for 3D opal-like magnetic PhC gives good results approving validity of the elaborated theory not only for two but also for three dimensions.

Relative phase shift between TE- and TM-modes that originates in the Voigt configuration shows similar sharp frequency dependence. This effect is analogous to the linear magnetic birefringence effect.

To conclude, magnetic PhC's evince giant magneto-optical effects (circular and linear birefringence) for radiation frequencies close to the extremum PB frequencies at the vicinity of high-symmetry points in the Brillouin zone. Besides, magnetic field can influence on PBG structure changing their width. All this proves that magnetic PhC's are of importance for light managing in modern devices of integrated optics.

This work is supported by RFBR (N° 01-02-16595, 02-02-17389, 03-02-16980).

References

1. E. Yablonovitch, Phys. Rev. Lett. **58**, 2059 (1987)
2. E. Yablonovitch et al., Phys. Rev. Lett. **61**, 2546 (1988)
3. S. John, Phys. Rev. Lett. **58**, 2486 (1987)
4. J.D. Joannopoulos, R.D. Meade, J.N. Winn, *Photonic Crystals: Molding the Flow of Light* (Princeton University Press, 1995)
5. V. Kuzmiak, A.A. Maradudin, Phys. Rev. B **57**, 15242 (1987)
6. E. Centeno, D. Felbacq, Phys. Lett. A **269**, 165 (2000)
7. C. Monat, C. Seassal, X. Letartre et al., Physica E **17**, 475 (2003)
8. M.D.B. Charlton, M.E. Zoorob, G.J. Parker et al., Mater. Sci. Engin. B **74**, 17 (2000)
9. T.A. Birks, D. Mogilevtsev, J. C. Knight et al., IEEE Photonics Technol. Lett. **11**, 674 (1999)
10. V. Berger, Phys. Rev. Lett. **81**, 4136 (1998)

11. K. Sakoda, K. Ontaka, Phys. Rev. B **54**, 5742 (1996)
12. T. Baba, M. Nakamura, IEEE J. Quantum Electr. **38**, 909 (2002)
13. P. Halevi, F. Ramos-Mendieta, Phys. Rev. Lett. **85**, 1875 (2000)
14. A. de Lustrac, F. Gadot, S. Cabaret et al., Appl. Phys. Lett. **75**, 1625 (1999)
15. S. Kim, V. Gopalan, Appl. Phys. Lett. **78**, 3015 (2001)
16. C.S. Kee, H. Lim, Y.K. Ha et al., Phys. Rev. B **64**, 085114 (2001)
17. D. Lacoste, F. Donatini, S. Neveu et al., Phys. Rev. E **62**, 3934 (2000)
18. B. Gates, Y.N. Xia, Adv. Mater. **13**, 1605 (2001)
19. X.L. Xu, G. Friedman, K.D. Humfeld et al., Adv. Mater. **13**, 1681 (2001)
20. E.L. Bizdoaca, M. Spasova, M. Farle et al., J. Magn. Magn. Mater. **240**, 44 (2002)
21. A. Figotin, I. Vitebsky, Phys. Rev. E **63**, 066609 (2001)
22. Y. Saado, M. Golosovsky, D. Davidov et al., Phys. Rev. B **66**, 195108 (2002)
23. M. Inoue, K. Arai, T. Fujii et al., J. Appl. Phys. **85**, 5768 (1999)
24. A.K. Zvezdin, Bulletin of the Lebedev Physics Institute (RAS) **37** (2002)
25. M. Levy, H. C. Yang, M.J. Steel et al., J. Lightwave Technol. **19**, 1964 (2001)
26. M.J. Steel, M. Levy, R.M. Osgood Jr., J. Lightwave Technol. **18**, 1297 (2000)
27. A.K. Zvezdin, V.A. Kotov, *Modern Magneto-optics and magneto-optical materials* (IOP Publishing, Bristol and Philadelphia, 1997)
28. J. Metzendorf, F.R. Kessler, Phys. Status Solidi (b) **71**, 237 (1975)
29. I.S. Grigoriev, *Hand-book Physical values* (Moscow, 1991)
30. K. Sakoda, *Optical properties of Photonic Crystals* (Springer, 2001)
31. M. Plihal, A. Shambrook, A.A. Maradudin, Opt. Commun. **80**, 199 (1991)
32. C. Koerdt, G.L.J.A. Rikken, E.P. Petrov, Appl. Phys. Lett. **82**, 1538 (2003)